

THE DE HAAS—VAN ALPHEN EFFECT IN ZINC IN PULSED MAGNETIC FIELDS. II

V. A. VENTTSEL', A. I. LIKHTER, and A. V. RUDNEV

Institute of High-pressure Physics, Academy of Sciences, U.S.S.R.

Submitted February 16, 1967

Zh. Eksp. Teor. Fiz. 53, 108—115 (July, 1967)

The frequencies of the de Haas—van Alphen effect in zinc in the (0001) plane are measured. The angular dependence of the effective mass of the “butterfly” is obtained. The problem of magnetic breakdown of the spin-orbit gap (modulation of amplitude of the “breakdown” frequency, increase of the Dingle factor in the breakdown region) is discussed.

WE have previously^[1] measured the areas of the extremal sections of the Fermi surface in zinc by the method of the de Haas—van Alphen effect in pulsed magnetic fields for the crystallographic planes (10 $\bar{1}0$) and (11 $\bar{2}0$). In this paper we present data on frequency measurements for the third principal crystallographic plane (0001), and also discuss the dependence of the oscillation amplitude on the temperature and on the magnetic field. From the frequency of the oscillations of the magnetic-susceptibility $F = \hbar c S_m / 2\pi e$ we can determine the area of the extremal cross section of the Fermi surface in the plane perpendicular to the magnetic field \mathcal{H} ^[2] (here F is in Oe and S_m in Å^{-2} , with $F = 1.045 \times 10^8 S_m$). In the resonant procedure employed by us, using a pulsed magnetic field^[3], the amplitude of the “splashes” is proportional to

$$w \sim T\mathcal{H}^{-1/2} \exp\left(-\frac{2\pi^2 mckx}{eh\mathcal{H}}\right) \left(\text{sh} \frac{2\pi^2 mckT}{eh\mathcal{H}}\right)^{-1},$$

where m is the effective mass of the electron and $x = \hbar/\pi k\tau$ is the Dingle factor, which takes into account the broadening of the levels as a result of scattering by impurities and by lattice imperfections, and τ is the relaxation time^[4,5]. The dependence of the amplitude on the temperature T and on the magnetic field \mathcal{H} make it possible to determine respectively the effective mass m and the Dingle factor x .

Zinc is a divalent metal with hexagonal lattice symmetry, and has in the almost-free electron model^[6,7] the Fermi surface shown in Fig. 1. Without allowance for the spin-orbit coupling^[8], zinc has a doubled Brillouin zone (first and second hole zone and third and fourth electron zone). The hole surface of zinc is a complicated multiply connected surface, called the “monster,” and the electron surface consists of a “lens” with center

at the point Γ , small “needles” on the vertical faces with center at the point K , and “shells” b on the faces HH with center at the points L . However, as shown in^[8-10], the spin orbit coupling lifts the degeneracy on the hexagonal plane (0001), leading to the existence of four single Brillouin zones. Small “pockets”^[11] remain in the first zone, and the hole surface^[12,13] in the second zone becomes open along [0001]. However, even a relatively weak field of 17.5 kOe^[13] causes breakdown of the spin-orbit gap, and the Fermi hole surface of zinc again goes over to a doubled zone. The presence of a spin-orbit gap in the third—fourth Brillouin zones causes four-wing “butterflies” c to be produced in the third zone in lieu of the

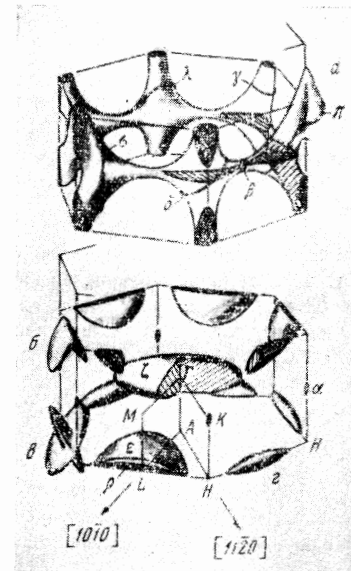


FIG. 1. Fermi surface of zinc for hole (top) and electron (bottom) surfaces with allowance for the spin-orbit gap. a – Element of hole surface in doubled Brillouin zone 1 – 2; b – surface of “shell” type in doubled Brillouin zone 3 – 4; c and d – surface of “butterfly” type in third zone and “cigar” in fourth zone with allowance for the spin-orbit gap.

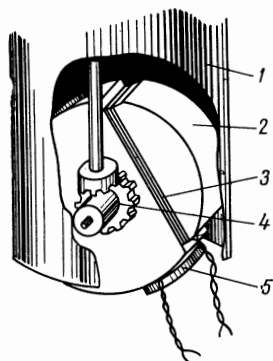


FIG. 2. Device for rotating the sample in the magnetic field.

“shells” b, and “cigars” d enter in the fourth zone. In ^[1] we observed the “butterfly” section in fields up to 70 kOe. It was of interest to investigate in greater detail the behavior of the frequencies connected with the “butterfly” near this direction, where, in our opinion, magnetic breakdown between the third and fourth zones comes into play. It is interesting to note that the “butterfly” cross section was not observed in either stationary fields in zinc ^[11,14] (these papers contain reviews of all the earlier experiments), or in pulsed fields in cadmium ^[15], metals having a similar electronic structure and an even larger spin-orbit gap ^[8].

EXPERIMENTAL TECHNIQUE

The first to measure the de Haas—van Alphen effect in pulsed magnetic fields was Shoenberg ^[16]; all the main methodological features of his technique are described in greatest detail in ^[3]. When a capacitor bank ($C = 2000 \mu\text{F}$, $U_{\text{max}} = 2700 \text{ V}$) is discharged through an inductance coil, a damped magnetic field $\mathcal{H} = \mathcal{H}_0 e^{-\delta t} \sin \omega t$ is produced in the latter ($\mathcal{H}_{\text{max}} \approx 100 \text{ kOe}$). The parameters \mathcal{H}_0 , δ , and ω are determined by the stored energy $CU^2/2$ and by the coil parameters, which are calculated by means of formulas contained in Champion's paper ^[17]. The field was calibrated against the variation of the change in the magnetic flux linking a coil with a known cross section NS. The solenoid was a multilayer coil of 0.8 mm diameter wire, 150 mm long, and with an inside diameter 21 mm (determined by the dimension of the rear part of the helium dewar). The number of turns in the coil was of the order of 2500, and the time required for the field to rise to \mathcal{H}_{max} was 14 msec.

Samples of a specified orientation were cut by the electric spark method, etched in HCl to the required dimension ($\sim 0.5 \text{ mm}$ diameter and $\sim 10 \text{ mm}$ length) and mounted in a holder on which lines were engraved corresponding to the positions

of the crystallographic axis. The samples were then inserted together with the holder inside a test coil consisting of two coaxial sections wound in opposite directions (to cancel out the signal proportional to $d\mathcal{H}/dt$). The coil was 8 mm long and of 3 and 0.8 mm outside and inside diameter, wound with PÉV-2 wire (0.02 mm diameter). The number of turns in the sections was ~ 3000 and ~ 1500 .

The test coil was placed with the sample 5 (Fig. 2) in a drum 2 secured inside a tube 1, and its axis could be rotated with the aid of a gear train 4 through an angle $\pm 30^\circ$ relative to the direction of the magnetic field. The angle of rotation was read on a dial placed on the cover, and was also determined by the voltage induced in coil 3, the axis of which was perpendicular to the axis of the test coil 5. The overall error in the determination of the angle did not exceed 2° . Inasmuch as the voltage of the trial coil always included a component proportional to $d\mathcal{H}/dt$ besides the component connected with the frequency of the de Haas—van Alphen effect, the signal from the test coil was fed to a preamplifier-filter, which transmitted only frequencies higher than 1 kHz. The signal was then fed to one of the inputs of a double-beam oscilloscope S1-18, and a field signal, picked off a 0.01-ohm resistance in the discharge circuit, was applied to the second input. In view of the complicated shape of the Fermi surface of zinc, many different extremal sections can

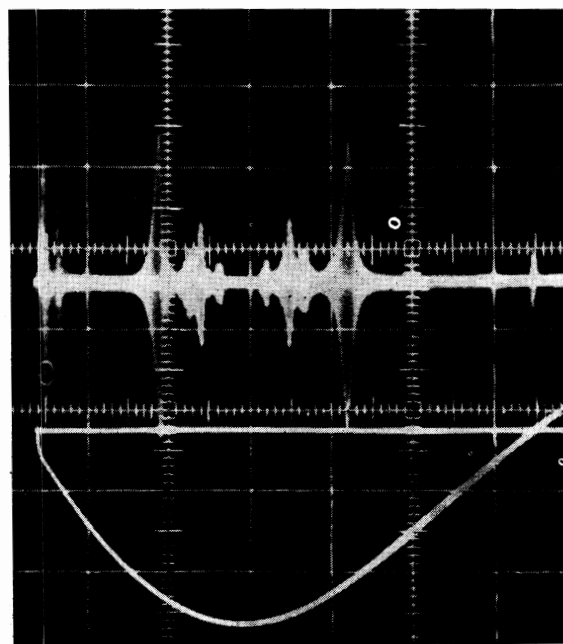


FIG. 3. Oscillogram of the dependence of $d_y/d\mathcal{H}$ and \mathcal{H} on the time for Zn-23 sample in the (0001) plane 8° from the $[11\bar{2}0]$ axis. $\mathcal{H}_{\text{max}} = 75 \text{ kOe}$.

be seen in any direction. A resonance method^[3] was used to resolve the individual sections. A typical oscillogram is shown in Fig. 3, where different "splashes" correspond to different extremal sections. The frequencies determined from the expression

$$F = \mathcal{H}^2 f (d\mathcal{H} / dt)^{-1},$$

where \mathcal{H} and $d\mathcal{H}/dt$ are taken at the instant of resonance and f is the resonant radiofrequency.

The purity of the samples can be characterized by the Dingle factor x . The value obtained by us for the section of the lens ζ in the $[10\bar{1}0]$ direction is $x = 0.65^\circ\text{K}$, demonstrating the high purity of the employed samples. The frequency measurements in^[1] and in the present paper were made on a large number of samples.

MEASUREMENT OF THE FREQUENCIES IN THE (0001) PLANE

The values of the frequencies F of the oscillations of the de Haas—van Alphen effect in the (0001) plane are shown in Fig. 4, and the amplitudes corresponding to these frequencies are shown in Figs. 5a and b.

The frequency A , corresponding to the section ζ of the "lens" in the center of the third Brillouin zone, and the frequency A' (its first harmonic), were observed for all values of the angles in this plane, and have a constant value (7.6×10^7 Oe for A and 15×10^7 Oe for A'), and also a fixed amplitude (as illustrated by Fig. 5b for the frequency A). By measuring the temperature dependence of the amplitude at these frequencies, we obtained the effective mass of the electrons, which for the

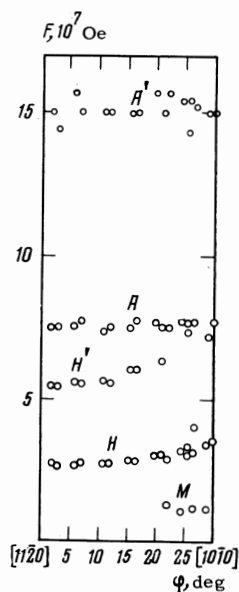


FIG. 4. Dependence of the frequency of the oscillations of the de Haas—van Alphen effect on the orientation of the field \mathcal{H} in the (0001) plane for sample Zn-23.

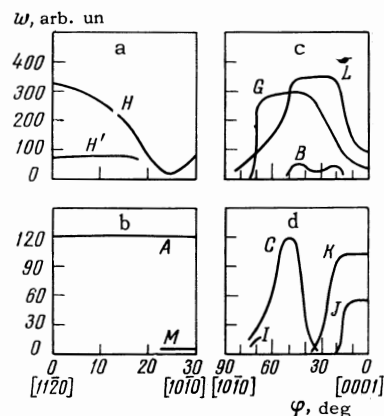


FIG. 5. Amplitudes of the oscillations of different frequencies of the de Haas—van Alphen effect as a function of the orientation of the field \mathcal{H} for the planes (0001) and $(11\bar{2}0)$ (in arbitrary units). The indices correspond to the notation of^[1] and of the present paper.

frequency A is equal to $0.54m_0$ in the $[11\bar{2}0]$ direction and $0.59m_0$ in the $[10\bar{1}0]$ direction; for the frequency A' in the same directions we obtained respectively $1.1m_0$ and $1.15m_0$. These data agree with the measurements of the effective mass by means of cyclotron resonance^[18] and confirm that A' is a harmonic of A . It is also seen from this that the effective-mass measurement accuracy is not worse than 5%.

The frequency H observed by us coincides fully with the frequency F_9 in^[14], ascribed to the section σ . As seen from Fig. 5a, the amplitude corresponding to this frequency is quite high in the $[11\bar{2}0]$ direction, reaches a minimum near 24° to the $[11\bar{2}0]$ axis, and increases somewhat in the direction of $[10\bar{1}0]$. The minimum of the amplitude is apparently connected with the attainment of the effective-mass value $m = 0.5m_0$. In addition, we observed the frequency H' , which we regard as the first harmonic of the frequency H . This follows not only from the multiplicity of the frequencies in the entire angle interval (up to 20°), but also from the fact that the effective mass for the cross section H' is double the mass for the section H . Thus, in the $[11\bar{2}0]$ direction $m/m_0 = 0.44$ for the frequency H and $m/m_0 = 0.92$ for the frequency H' . Finally, in the (0001) plane there is one more frequency, denoted by us by M . This frequency has a value 1.1×10^7 Oe and is observed near the $[10\bar{1}0]$ direction. The amplitude corresponding to this frequency is very small (see Fig. 5b), and the effective mass for it amounts to $(0.31 \pm 0.05)m_0$. The absence of an angular dependence of this frequency does not make it possible to make any statements concerning its origin.

Table I

Symbol	Designation of present paper and [1]	Designation of [18]	Orbit on Fig. 1	Symbol	Designation of present paper and [1]	Designation of [18]	Orbit on Fig. 1
Δ	A	a	ζ	\bullet	I	—	—
\circ	C	—	ϵ	\blacktriangle	L	d	γ
\square	G	c	δ		M	—	—
\times	H	e	σ				

AMPLITUDE MEASUREMENTS IN $(11\bar{2}0)$ PLANE

Figures 5c and d show the angular dependence of the amplitude of the “splashes” of the observed frequencies in the $(11\bar{2}0)$ plane, and Fig. 6 shows the quantities of the effective masses obtained from cyclotron-resonance data [18] (solid lines) as well as our experimental data for the angles 50 – 70° . The symbols are defined in Table I.

It was proposed in [1] that the frequencies of series C and I correspond to the section of the “butterfly” in the third zone. Since such a section was not observed earlier in either zinc or cadmium, it was of interest to measure the effective mass for the section connected with the frequency C. The measured m/m_0 for this section did not agree with any of the values of the effective mass obtained by cyclotron resonance [18], but at the same time it yielded a rather characteristic picture, evidencing that the frequency C belongs to the section ϵ of the “butterfly.” This section has $m/m_0 = 0.9$ for $\varphi = 65^\circ$, which is close to unity—the expected value for a circular cross section in the almost-free-electron model, and decreases with increasing distance from this direction, in both sides, which is also in agreement with the predictions of the almost-free-electron model. Thus, $m = 0.76 m_0$ for $\varphi = 70^\circ$ and $0.6 m_0$ for $\varphi = 50^\circ$.

The decrease in the amplitude of the oscillations of frequency C at angles larger than 50° , and the vanishing of these oscillations at 75° , can be attributed to the occurrence of magnetic breakdown of the spin-orbit gap, as was indeed proposed in [1]. In the breakdown there should be observed frequencies corresponding to both the “butterfly” and the “cigar” as well as corresponding to the “shell.” If we assume that the section of the “cigar” is equal to the same value as near the $[0001]$ (the frequency K in [1] is 1.1×10^7 Oe near this direction), then the section of the “shell” should be equal to half the sum of these values, that is, $F_C/2 + F_K/2 = 2.8 \times 10^7$ Oe. It was observed experimentally that in the considered angle interval there are seen strong beats of the

frequencies close to the indicated values $F \approx 1.1 \times 10^7$ Oe (L, section γ) and $F \approx 2.8 \times 10^7$ Oe (G, section δ). The frequency I ($F_I = 1.7 \times 10^7$ Oe) is observed in a small angle interval near 70° , and cannot be attributed to the “shell” section, since this frequency corresponds to half the difference of the frequencies C and K. It can be assumed that such a section corresponds to the section of “butterflies” situated on the other edges HH of the Brillouin zone. For these, the area of the central section in the free-electron model is of the order of 0.25 \AA^{-2} , which can, with allowance for the lattice potential, yield a value close to that obtained in the experiment, but the mass for such an orbit should be $\sim 0.38 m_0$, which is much lower than the observed value $(0.5 \pm 0.02) m_0$. For the “shell” in the same place of the Brillouin zone, according to estimates made in the almost-free-electron model, we have $S = 0.15 \text{ \AA}^{-2}$ and $m/m_0 \approx 0.25$, so that the frequency I can hardly be assigned to such sections.

It can be assumed, however, that the frequency I is the result of an oscillatory dependence of the gap E_g between the “butterfly” and the “cigar” on \mathcal{H} (the same idea is the basis of an explanation of the “giant” oscillations of magnetoresistance in zinc [19,20]). Owing to the presence of Landau levels, the distance between which is $\mu\mathcal{H}$, it is natural to expect the breakdown probability [7,9,21], defined as $\exp(-E_g^2/\mu\mathcal{H}E_F)$, to depend on the

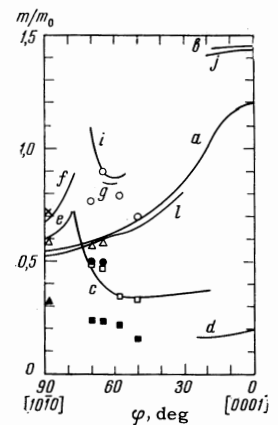


FIG. 6. Angular dependence of the effective masses in the $(11\bar{2}0)$ plane as obtained from cyclotron-resonance data [18] (solid lines) and in the present work.

Table II. Behavior of the Dingle factor in the region of magnetic breakdown of the spin-orbit gap.

φ , deg	Orbit			
	C	G	I	L
50	0.7±0.05	—	—	—
57.5	1.2±0.05	2.3±1	—	3.0±0.5
65	1.9±0.05	1.8±1	2.8±0.05	3.0±0.75
70	1.5±0.05	1.8±1	1.8±0.05	4.8±1

field in nonmonotonic fashion if E_g is commensurate with $\mu\mathcal{H}$, which does take place in general ($E_g \sim 0.03$ eV^[8] and $\mu\mathcal{H} \sim 0.002$ eV). Since the frequencies of the “butterfly” and the “cigar” and the effective masses corresponding to them are of the same order, the oscillating width of the gap will depend on $\mu_C\mathcal{H}$ and $\mu_K\mathcal{H}$ and this can cause the amplitude of the oscillations corresponding to the breakdown frequency of the “shell” to be modulated, the modulation frequency being equal to half the difference between the initial frequencies $F_C/2 - F_K/3 = 1.7 \times 10^7$ Oe. It is interesting to note that the amplitudes for the frequencies I and G have nearly the same dependences on the temperature and on the magnetic field (Fig. 6 and Table II).

As indicated above, the Dingle factor describes the electronic-level broadening due to scattering by impurities and the consequent finite relaxation time τ . The amplitude factor can have the form $\exp(-2\pi/\omega\tau)$ and the form $\exp(-\mathcal{H}_x/\mathcal{H})$, which is more convenient for an experimental determination ($\mathcal{H} = 2\mathcal{H}^2$ mck/ $\hbar e$). Since usually $\mathcal{H}T/\mathcal{H}$ is large, we can replace the hyperbolic sine by an exponential, and the field dependence of the amplitude will take the form $w \sim \mathcal{H}^{-1/2} \exp(-\mathcal{H}(T+x)/\mathcal{H})$. By plotting in $w\sqrt{\mathcal{H}}$ as function of $1/\mathcal{H}$, we obtain a straight line with slope $\mathcal{H}(T+x)$, and from it the value x of the Dingle factor, in degrees K, listed in Table II for the frequencies C, G, I, and L in the angle interval 50–70°.

For the frequencies G and L, the obtained values of the Dingle temperature have a large scatter, and are therefore only of qualitative interest. Attention is called to the fact that x is large for all frequencies in the magnetic-breakdown region, although it amounts to 0.65°K for A in the $[10\bar{1}0]$ direction and 0.7°K for C at 50°.

Unfortunately, the theory does not yield the dependence of τ on the anisotropy of the metal and, as follows from^[5], τ is isotropic for the quadratic dispersion law that holds in the angle inter-

val under consideration for the frequency C. In the case of magnetic breakdown, the amplitude of the oscillations is proportional to the probability of finding the electron on a given trajectory, and this probability is of the form $\exp(-2\pi/\omega\tau_0)$, where $1/\tau_0$ is reported by different authors to have the form $E_g^2/\hbar E_F$, disregarding some factors. If we denote, by analogy with the Dingle factor x , the quantity $\hbar/\pi k\tau_0$ by y and recognize that the probability of existence of a breakdown trajectory is equal to $\exp(-2\pi n/\omega\tau_0) = \exp(-n\mathcal{H}y/\mathcal{H})$, where n is the number of passages of the electron through the gap E_g , then the “effective Dingle factor” will be equal to $x + ny$. Since we have $n = 2$ for the breakdown frequency I, it follows that, by assuming x to be independent of the orientation and equal to $\sim 0.7^\circ\text{K}$ for all cross sections, we obtain $y \approx 1^\circ\text{K}$ for $\varphi = 65^\circ$. Hence $1/\tau_0 \approx 4 \times 10^{11}$ sec⁻¹ and from the relation $1/\tau_0 = E_g^2/\hbar E_F$ we get that the spin-orbit gap should not exceed $E_g \lesssim 0.05$ eV, in agreement with the calculations of Cohen and Falicov^[8]. For $\varphi = 70^\circ$, we have $y = 0.5^\circ\text{K}$, which should offer evidence, within the framework of our assumptions, that the dependence of $1/\tau_0$ is more complicated, as shown for example, in the paper by Harrison^[7].

In the case of a “butterfly” orbit, the dependence of the “effective Dingle factor” will be more complicated, since the probability of existence of such an orbit is $(1 - \exp(\mathcal{H}y/\mathcal{H}))^2$. Since $\mathcal{H}y/\mathcal{H} \sim 1$, it is difficult to represent the “effective Dingle factor” in a form convenient for the interpretation of the experimental values. However, the numerical value of y of the “butterfly” agrees with the value obtained above.

Thus, a qualitative consideration of the dependence of the amplitude on the magnetic field leads to a conclusion that a connection exists between the measured Dingle factor and the presence of the magnetic breakdown, which in turn makes it possible to estimate the magnitude of the spin-orbit gap.

In conclusion, the authors consider it their pleasant duty to thank L. F. Vereshchagin for continuous interest in the work, A. P. Kochkin for valuable discussions, G. P. Pushtarik for high grade x ray orientation, and V. M. Mal'tsev for excellent performance of complicated mechanical operations.

¹V. A. Venttsel', A. I. Likhter, and A. V. Rudnev, ZhETF Pis. Red. 4, 216 (1966) [JETP Lett. 4, 148 (1966)].

- ²I. M. Lifshitz and A. M. Kosevich, Zh. Eksp. Teor. Fiz. **29**, 730 (1955) [Sov. Phys.-JETP **2**, 636 (1956)].
- ³D. Shoenberg, Phil. Trans. Roy. Soc. **A255**, 85 (1962).
- ⁴R. B. Dingle, Proc. Soc. **A211**, 517 (1952).
- ⁵Yu. A. Bychkov, Zh. Eksp. Teor. Fiz. **39**, 1401 (1960) [Sov. Phys.-JETP **12**, 971 (1961)].
- ⁶W. A. Harrison, Phys. Rev. **118**, 1190 (1960).
- ⁷W. A. Harrison, Phys. Rev. **126**, 497 (1962).
- ⁸M. H. Cohen and L. M. Falicov, Phys. Rev. Lett. **5**, 544 (1960).
- ⁹M. H. Cohen and L. M. Falicov, Phys. Rev. Lett. **7**, 231 (1961).
- ¹⁰L. M. Falicov and M. H. Cohen, Phys. Rev. **130**, 92 (1963).
- ¹¹A. S. Joseph and M. L. Gordon, Phys. Rev. **126**, 489 (1962).
- ¹²W. A. Reed and G. F. Brennert, Phys. Rev. **130**, 565 (1963).
- ¹³R. W. Stark, Phys. Rev. **135**, A1698 (1964).
- ¹⁴R. J. Higgins, J. A. Marcus, and D. H. Whitmore, Phys. Rev. **137**, A1172 (1965).
- ¹⁵A. D. C. Grassie, Phil. Mag. **9**, 847 (1964).
- ¹⁶D. Shoenberg, Nature **170**, 569 (1952).
- ¹⁷K. S. W. Champion, Proc. Phys. Soc. **B63**, 795 (1950).
- ¹⁸M. P. Shaw, P. J. Sampath, and T. G. Eck, Phys. Rev. **142**, 399 (1966).
- ¹⁹R. W. Stark, Phys. Rev. Lett. **9**, 492 (1962).
- ²⁰Yu. P. Gaïdukov and I. P. Krechetova, Zh. Eksp. Teor. Fiz. **49**, 1411 (1965) [Sov. Phys. **22**, 971 (1966)].
- ²¹E. J. Blount, Phys. Rev. **126**, 1636 (1962).

Translated by J. G. Adashko